A clinically applicable model to estimate the opposing muscle groups contributions to isometric and dynamic tasks

Pauline Gerus[1], Guillaume Rao[1], Thomas S. Buchanan[2], and Eric Berton[1]

[1]*Institute of Movement Sciences E-J Marey, UMR CNRS 6233, Aix-Marseille University , Marseille, France;*

[2]*Center for Biomedical Engineering Research, Dept. of Mechanical Engineering, University of Delaware, Newark, DE 19716, USA.*

Running Head: A clinical model to estimate muscle group contributions

Address correspondence to:

Pauline GERUS

Institute of Movement Sciences EJ. Marey, UMR CNRS 6233

Aix-Marseille University

Parc Scientifique et Technologique de Luminy,

163, Avenue de Luminy,

13288 Marseille cedex 09, France

Phone : + 33 491 17 04 78

Fax : + 33 491 17 22 52

Email : pauline.gerus@univmed.fr

Abstract

This paper presents an EMG-to-moment optimization model suitable for clinical studies to estimate the contribution of agonist and antagonist muscle groups to the net ankle joint moment during dynamic and isometric tasks. The proposed EMG-to-moment model took into account realistic muscle properties such as the electromechanical delay, and a force-length-velocity relationship with subject specific muscle anthropometric data. Subjects performed isometric ankle plantar-flexion (fixed-end contraction) and dynamic tasks (heel-raise) in two positions, seated and upright. Two models were compared: the proposed EMG-to-moment model calibrated on eight dynamic and isometric tasks (Model 8-tasks) and on two dynamic tasks (Model 2-tasks), and a published reference model. First, each model was calibrated at the ankle joint on ten subjects by adjusting individual set of parameters to estimate the muscle groups contributions. Then, the model was used to predict the ankle net joint moment. The model developed in this study showed good prediction. The Model 8-tasks predicted net joint moment with an average RMS error of 6.11 ± 4.41 Nm and a mean R^2 of 0.67 ± 0.26 across dynamic and isometric tasks. The proposed EMG-to-moment model was simple and required few calibration tasks without oversimplifying muscle properties, satisfying requirements for clinical settings.

Key terms: EMG-to-moment optimization model, electromechanical delay, force-length-velocity relationship, muscle group moment, ankle joint

INTRODUCTION

The estimation of muscle forces and moments could help clinicians to investigate and treat musculoskeletal disorders [5,9,38]. However, measurements of *in vivo* muscle forces are invasive and limited to superficial structures such as Achilles' tendon [11]. From a mechanical point of view, inverse dynamics only allows one to estimate the resultant action of all the muscles crossing a joint. However, due to the presence of muscular redundancy, an assessment of the contribution of each muscle or muscle group to the net joint moment is difficult. This makes the development of approaches to estimate muscle forces that are simple enough to be readily used in a clinical setting a difficult task. The co-contraction level computed from the contribution of the agonist and antagonist muscle groups to the net joint moment provides useful information for clinicians to study adaptive changes in motor strategies with musculoskeletal disorders. For example, the presence of adaptive changes in motor strategies has been shown for patients with an anterior cruciate ligament deficiency. This increase in co-contraction level was associated with an active joint stabilization to compensate for the loss of passive stability [9]. The co-contraction level could be used to evaluate clinical interventions and functional recovery during rehabilitation program.

The magnitude of the moment exerted by a muscle at a joint results from both the moment-arm and the muscle force. The moment arm of the muscle-tendon complex changes as a non-linear function of the joint angle [22]. The muscle force generated by the contractile elements in the muscle depends on the length and velocity of the muscle fibers through non-linear relationships [13,16]. This muscle force is transmitted to bones via tendinous tissues (tendons and aponeurosis) and is influenced by the mechanical properties of these elements in series [35]. The muscle force also depends on the level of activation with a temporal phase shift due to the electromechanical delay (EMD) between the activation and effective force production. Experimentally, this level of activation can be estimated using electromyographic (EMG) data [28]. Because of these factors, the estimation of the muscle moment from EMG data is very non-linear and thus not trivial. Hence, the preceding factors justify the development of an EMG-to-moment model, as the co-

activation itself may give erroneous information on muscle groups influences.

To estimate the muscular contributions to joint moments from EMG data, the steps outlined above (from muscle activation to moment production) need to be taken into account. Rao et al. [32] developed an EMG-to-moment model based on the model of Amarantini and Martin [2] which used optimization procedures to estimate the contributions of the agonist and antagonist muscle groups to the net joint moment during dynamic tasks. The design of this model made it suitable for clinical applications without requiring a large number of experimental steps. However, from the EMG data of selected leg muscles, the muscle contraction dynamics was introduced by linear moment-angle and moment-velocity relationships without introducing the electromechanical delay during the EMG processing contrary to the approach taken by other models [4,10].

Another more complex EMG-driven model developed by Buchanan et al. [4] allows one to estimate the force produced by each muscle incorporating more physiological and mechanical muscle properties that will be briefly presented. First, within the "muscle activation dynamics" step [40], the muscle activation was estimated from the EMG data with the introduction of the EMD. Then, muscle anthropometric data (length and velocity of muscle fibers and muscle-tendon moment arms) which directly influence the moment production capacity, were estimated from an anatomical model. Muscle forces were deduced from a Hill-type model with experimentally obtained force-length and force-velocity relationships[13,16]. This model led to very good moment predictions, thus increasing the confidence in the results [26]. Nevertheless, the complexity of the model and the large number of required calibration steps could be detrimental for use in clinical studies. The choice of a model to estimate the muscle (or muscle group) moments strongly depends on its application. For clinicians, the model should be easy to implement [32] without neglecting muscle physiological properties [4].

The estimation of muscle force by EMG-driven models was often restricted to either isometric [21,24] or dynamic tasks [9,31] but few models were tested during both isometric and dynamic conditions (only during calibration process [26]). Given that the knowledge of muscle moments could be crucial for clinicians,

the model should be implemented for any type of contraction (i.e., isometric, concentric, and eccentric).

The purpose of the present study was to develop an EMG-to-moment optimization model for use in clinical studies to estimate the contributions of agonist and antagonist muscle groups to the net joint moment for isometric and dynamic conditions, using the ankle joint as example. To this aim, the proposed model used the approach of Rao et al. [32] with notable changes. These improvements were made to include realistic muscle properties in order to provide a model that can be implemented over a wide range of contractions (i.e., isometric, concentric, and eccentric) without increasing the number of experimental steps. Especially, the electromechanical delay and a force-length-velocity relationship with anthropometric data were incorporated as inputs. After the model calibration process, we examined the ability of model to predict net joint moments across various tasks. The proposed EMG-to-moment model calibrated on eight dynamic and isometric tasks (Model 8-tasks), and on two dynamic tasks (Model 2-tasks) was compared to the approach of Rao et al. [32] calibrated on two dynamic tasks.

METHODS

Subjects

Ten healthy males (age 25.3 ± 2.4 years, body mass 74.6 ± 9.1 kg, height 1.76 ± 0.04 m) participated in this study. The protocol of this study was approved by the University Review Board and all participants gave informed written consent.

Experimental design and acquisition

Subjects stood with their right foot on a force platform and performed three ankle plantar flexion maximum isometric voluntary contractions (MIVC) during 5s with a rest time of 2 minutes between each trial. Verbal encouragement was provided to obtain maximal effort during MIVC. This task was chosen only to obtain their maximal voluntary force used as reference for the next conditions. After MIVC, subjects then performed 2 sets of 8 tasks: three series of isometric contractions (1-2) fifteen sinusoidal oscillations (between 10-30% and 30-50% of maximal voluntary force (MVF)) at a rate of 1 Hz, (3) ramp

increase in force (0 to 60 % MVF in 5s) and as dynamic tasks, fifteen cycles of heel-raise (rise up and down on toes) at a rate of 1 Hz, each under two configurations, seated and standing. The first set of tasks was used to calibrate models, while the second set was used to evaluate the models by predicting net joint moment. For isometric tasks, subjects had a visual feedback of the vertical ground reaction force and were asked to follow a target displayed on a computer screen. The subject position was fixed using a rigid experimental apparatus designed to minimize movements of individual body segments (Fig. 1). The isometric condition was defined as a fixed-end contraction where the muscle-tendon complex was held at constant length. These tasks were chosen to encompass a wide range of contractile conditions [26] while being suitable for clinical testing.

[Insert figure 1]

All testing procedures were performed on a force platform (AMTI, Model BP6001200, Watertown, USA) that recorded ground reaction forces at 1560 Hz. Kinematic data were recorded synchronously by six-camera VICON (Vicon Motion System, Lake Forest, CA) at 120 Hz tracking twelve markers attached to the fifth and first metatarsal heads, the calcaneum, the lateral and medial malleoli, the fibula head, the lateral and medial condyles of the femur, the greater trochanter only for the right leg, and the right and left anterior superior iliac spines and the sacrum. A fourth-order, zero-lag Butterworth filter was used on raw kinematic and dynamic (i.e., ground reaction forces) data with a 6 Hz and 10 Hz cut-off frequency, respectively.

EMG signals were recorded at 2000 Hz (MP150, Biopac System Inc., Goleta, CA, gain=5000, CMRR=100db, bandwidth=10-500 Hz, power line frequency = 50 Hz) using Ag/Ag-Cl bipolar surface electrodes (EL503, Biopac System Inc., Goleta, CA) placed over the muscles with a 2cm inter-electrodes distance according to recommendations of the SENIAM group [15]. The tibialis anterior was chosen to represent the ankle dorsiflexor group (DF) while the gastrocnemius lateralis, the gastrocnemius medialis and the soleus represented the ankle plantar flexor group (PF). These muscles were chosen as they represented the main actuators in dorsi/plantar flexion movements at the ankle joint [12].

Data processing

Using OpenSim (Simtk, Standford, USA), a generic lower limb anatomical model including bones and four musculotendon actuators (tibialis anterior, gastrocnemius lateralis, gastrocnemius medialis, and soleus) was developed based on the work of Delp [6]. First, the generic model was scaled to match the anthropometric characteristics of each individual subject using the kinematic data obtained during static upright standing. The coordinates of each marker were then used as input to estimate muscle fiber lengths and flexion-extension moment arms for each trial (more information in Delp et al. [5]). The muscle fiber velocity was obtained by time differentiating the muscle fiber length obtained previously.

The ankle net joint moment (*M*) was computed by solving the inverse dynamics problem using body segment parameter data [41] at each time step, *t*. The net joint moment was considered to be equal to the sum of the moments developed by the PF and DF muscle groups.

The MVIC tasks were used to estimate the EMD for each subject. The EMD was computed on MVIC trials as the time difference between the onset of EMG activity filtered at 50 Hz and full wave rectified, and the onset of raw vertical force. These onsets were defined as the time instants where the signal was 2 SDs higher than the mean resting activity [17,25]. In the current study, the EMD mean value was 83.6 ms (± 18.0 ms). The EMD was taken into account by using a controlled temporal shift obtained from a forward Butterworth filter of specific order and cut-off frequency [29]. The approximate time delay introduced by a forward Butterworth filter for specific cut-off frequency and order values could be estimated [29]. In the modified model, the value of cut-off frequency was fixed at 2.5 Hz according to the recommendation of the Model Rao et al. (further named Model RAB) [32]. Given the formulation given by Manal and Rose [29], using a 2nd order filter the resulting temporal shift was 90 ms, close to the mean EMD found in this study. In order to be used in clinical settings, no normalization of the EMG data was necessary.

The cycles were selected based on the maximal values of the vertical force and ankle angle respectively for the isometric and dynamic tasks. The data points between 10 and 60% of MVF of a single

ramp isometric contraction were normalized in time from 0% to 100% and used as input to the model. The remaining input data of model (i.e., kinematics, kinetics, EMG, moment arms, fiber lengths and velocities) were normalized in time from 0% to 100% of the cycle duration and then averaged over ten cycles after removing the first three and last two cycles. This was done to ensure the data were cyclical and not influenced by start-up and winding-down effects. In addition, this resulting number of cycles was sufficient to obtain reliable EMG data [37]. All data were re-sampled to obtain 25 points for each task.

Model descriptions

First, the EMG-to-moment optimization model developed in this study to estimate the contribution of agonist and antagonist muscle groups to the net joint moment will be presented. This model includes electromechanical delay during EMG processing as well as a force-length-velocity relationship combined with anthropometric data (muscle fiber length, muscle fiber velocity, and moment arm of muscle-tendon complex) and further represented by a single variable $\overline{\varphi}_i\ (t)$. This model was based on the approach described by Rao et al. [32]. Thus, in a second part, the model of Rao et al. [32] will be described.

The EMG-to-moment model developed in this study, gave the following optimization problem:

find, α_i , $w_i\ (t)$ and G_l with i= *{TA, GL, GM, SL}* and l=*{DF, PF}* that

minimized: $$C = \frac{1}{2}\sum_t (M(t) - \hat{M}(t))^2 \quad (1)$$

where : $$\hat{M}(t) = \sum_i (G_l\ \alpha_i\ w_i(t)\ rEMG_i\ (t)\ \overline{\varphi}_i(t)) \quad (2)$$

subject to: $$\begin{cases} 0.5 < G_l < 1.5 \ for\ \ l = \{ PF \} \ \ and \ \ -1.5 < G_l < -0.5 \ for\ \ l = \{ DF \} \\ 0 < w_i < 1 \ \ for\ \ i = \{ GL, GM, SL \} \ and \ \ w_i = 1 \ \ for\ \ i = \{ TA \} \\ \alpha_i > 0 \qquad\qquad for\ \ i = \{ TA, GL, GM, SL \} \end{cases} \quad (3)$$

In Eq. (1), $\hat{M}$ represents the net joint moment estimated by the model, while M is the moment computed from inverse dynamics. In Eq. (2) $rEMG_i(t)$ is the full-wave rectified, filtered and temporally shifted EMG of each muscle (Forward Butterworth, 2nd order, 2.5 Hz cut-off frequency). For each muscle,

the constant α_i represents the linear relationship between EMG and moment in isometric condition. $w_i\,(t)$ represents the relative contribution of each muscle to the total moment of muscle group. Opposite to the other adjustable parameters (α_i and G_l), the $w_i\,(t)$ parameter was optimized for each task. G_l represents the gain of each muscle group, and allows for adapting the maximal isometric force for each subject [3,13]. The positive or negative sign defines the muscle action: according to our convention, M_{DF} is positive and M_{PF} is negative. $\overline{\varphi}_i\,(t)$ represents the moment production capacity of each muscle depending on its specific length, velocity, and moment arm (Eq. 4).

$$\overline{\varphi}_i(t) = \overline{\gamma}_i(t).\overline{d}_i(t) \tag{4}$$

where $\overline{\gamma}_i(t)$ represents the normalized capacity of muscle force production (Eq. 4) and $\overline{d}_i(t)$ the normalized moment arm. For each muscle, the moment arm values at each time *t* were normalized by the maximum moment arm value in the range of ankle active motion (-35° and 22°, with 0° = neutral position and positive = *DF*) [1].

$$\overline{\gamma}_i(t) = \overline{f}(v_i(t)).\overline{f}((l_i(t)) \tag{5}$$

where $\overline{f}((l_i(t))$ stands for the active force depending on the muscle fiber length [13] and $\overline{f}(v_i(t))$ stands for the normalized force depending on the muscle fiber velocity [34]. The active force length relationship was normalized between 0 and 1 while the force-velocity curve evolved between 0 (maximal concentric contraction) and 1.8 (maximal eccentric contraction). Considering the ankle range of motion, the passive contribution of the force-length relationship was low [33]. Moreover, the muscles studied (gastrocnemius lateralis, gastrocnemius medialis, soleus and tibialis anterior) presented a high ratio between the tendon length (tendon and aponeurosis) and muscle fiber length. Thus, the passive force due to the parallel elastic component of Hill-type model could be neglected [41]. The corresponding variable ($\overline{\gamma}_i(t)$) could be represented as a 3D surface with normalized force production capacity depending on fiber length and velocity.

The model developed in this study was based on the one described by Rao et al. [32]. Only a brief description of this model is given here:

The contributions of the agonist and antagonist muscle groups to the net joint moment were estimated by solving the following optimization problem:

find α_i, $w_i(t)$, β_j *and* δ_j with i= {*TA, GL, GM, SL*} and j= {*a, k*} that

$$\text{minimize:} \quad C = \frac{1}{2}\sum_t (M(t) - \hat{M}(t))^2 \tag{6}$$

$$\text{with :} \quad \hat{M}(t) = \sum_i (\alpha_i . w_i(t) . rEMG_i(t))^T . [1 + E.(\beta_j . \Delta\theta_j) - E.(\delta_j . \dot{\theta}_j)] \tag{7}$$

$$\text{subject to:} \quad \begin{cases} \alpha_i > 0 \quad for \quad i = TA \quad and \quad \alpha_i < 0 \quad for \quad i = GL, GM, SL \\ \beta_j \quad and \quad \delta_j > 0 \\ 0 < w_i(t) < 1 \end{cases} \tag{8}$$

In Eq. (6), $rEMG_i$ represents the EMG signals of the major muscles filtered by a zero-lag filter (Butterworth, 4th order, 2.5 Hz cut-off frequency). The moment-angle and the moment-velocity effects are represented by two constants, β and δ, for each joint (j), with *a* and *k* representing the ankle and knee joints, respectively. Change in angle ($\Delta\theta_j$) and angular velocity ($\dot{\theta}_j$) were computed for the ankle and knee joints according to [39]. The biarticularity of the gastrocnemius muscles is taken into account by the matrix E [2].

Calibration and prediction process

In order to be used to predict the contribution of agonist and antagonist muscle groups to the net joint moment, the model first had to be calibrated. A summary of the parameters used in the present study is presented in Table I. The calibration process on both isometric and dynamic tasks could not be achieved for the Model RAB. Thus, in order to compare the Model RAB and the modified model, two different calibrations were performed. First, the modified model was calibrated using eight tasks (further named Model 8-tasks); isometric sinusoidal contractions across two ranges of force, one isometric ramp and one dynamic heel-raise task, each performed in two configurations, seated and standing. Then, the modified

model (named Model 2-tasks) as well as the Model RAB were calibrated for the two dynamic heel-raise tasks only. The optimization procedure was solved using a Sequential Quadratic Programming method (Matlab Optimization Toolbox).

Once the calibration process was successfully completed, the second set of tasks was used to predict the net joint moments over several tasks. These data combined with the set of optimized parameters obtained after the calibration phase were used to compute the ankle net joint moment. Model 8-tasks was used for moment predictions on all eight tasks. Model 2-tasks as well as the Model RAB were used to predict moments for the two dynamic tasks.

[Insert Table I]

Data analysis

A coefficient of determination (R^2) was used to indicate the linear relationship between the predicted moment and the moment computed by inverse dynamic for the corresponding task. A Root Mean Square value (Eq. 11) was also computed to indicate the magnitude of the errors [26] over each models (i.e., the Model RAB *vs.* Model 8-tasks *vs.* Model 2-tasks).

$$RMS_{error} = \left(\frac{1}{n} . \sum_{i=1}^{n} (M(t_i) - \hat{M}(t_i))^2 \right)^{1/2} \quad (11)$$

Where n represents the number of sample.

Statistics

Two-factor (*muscle* and *position*) Analysis of Variance (ANOVA) with repeated measures was conducted on mean values of $\overline{\varphi}_i(t)$ averaged across both isometric and dynamic tasks and amplitude (max value – min value) values of $\overline{\varphi}_i(t)$ obtained on dynamic task only. Indeed, concerning the amplitude of $\overline{\varphi}_i(t)$, this value was null for the isometric condition since there was no joint movement..

All following parameters were averaged across seated and standing positions. Following the

calibration step, a two-factor (*model* and *muscle*) ANOVA was conducted on the muscle gain (α_i). Concerning the ability of moment prediction, a one-factor (*model*) ANOVA was used to compare the mean value of RMS_{error} and R^2 averaged across tasks for the different models.

The outputs of the different models were the contributions of the plantar flexor and dorsiflexor muscle groups to the net joint moment, M_{PF} and M_{DF}, respectively. One-factor (*model*) ANOVA was conducted on the mean value of these variables estimated for the two dynamic tasks. A significance level of 0.05 was used for all comparisons and Newman-Keuls post-Hoc testing was used whenever necessary.

RESULTS

Model Input

For all conditions, the ankle joint angles ranged from 22.4° (± 7.0°) to -26.4° (± 7.6°) where 0° was neutral position. For the seated position, the mean value of the knee joint angle was (91.0° ± 7.6°) and (5.9° ± 5.9°) in the upright position where 0° was full extension.

A *muscle* effect ($F_{3,57}=55.43$; $p<0.05$) for the mean value of the moment production capacity, ($\overline{\varphi}_i^m$ variable) was found (Fig. 2). A *position* effect ($F_{1,19}=84.10$; $p<0.05$) for the mean value of $\overline{\varphi}_i^m$ was found. For both gastrocnemii, $\overline{\varphi}_i^m$ was smaller in the seated position than upright position. $\overline{\varphi}_i^m$ was higher for soleus than gastrocnemii in the seated position. The ANOVA showed that the amplitude of $\overline{\varphi}_i^m$ for the dynamic task depended on *muscle* only ($F_{3,27}=53.59$; $p<0.05$). The smallest amplitude was the tibialis anterior (0.56 ± 0.13) and the highest was the soleus (1.02 ± 0.21). Gastrocnemius lateralis (0.84 ± 0.19) and medialis (0.86 ± 0.22) were statistically different than values for the tibialis anterior and soleus.

[Insert figure 2]

Model Calibration

For Model 8-tasks, the calibration process for each subject was performed on eight tasks (i.e., isometric sinusoidal contraction (two ranges of forces), isometric ramp and dynamic heel-raise in two

positions) while the Model RAB and Model 2-tasks were calibrated using only two dynamic tasks. ANOVAs indicated significant effects of *model* and *muscle* factors on muscle gain (α). Post-Hoc tests indicated that the values from Model 8-tasks (modified model calibrated on eight tasks) were higher than the values of the Model 2-tasks and Model RAB calibrated on two dynamic tasks. In addition, Post-Hoc tests indicated that the smallest gain was the tibialis anterior and the highest was the soleus. Both gastrocnemius lateralis and medialis were different from tibialis anterior and soleus.

Model prediction

For the dynamic tasks the different models predicted different net joint moments (Fig. 3). Concerning the moment prediction of the different models on dynamic tasks, an ANOVA indicated a significant ($F_{2,18}=14.06$; $p<0.05$) effect of *model* factor on R^2 values averaged of seated and standing tasks. Post-Hoc tests indicated the R^2 values for the Model RAB (0.28 ± 0.24) were smaller than those of the modified model calibrated on two (0.53 ± 0.25) and eight tasks (0.46 ± 0.25). No significant effect of *model* was obtained on RMS_{error} ($F_{2,18}=0.93$; $p<0.05$).

[Insert figure 3]

The modified model was able to predict net moments at the ankle for a single subject across all isometric tasks (Fig. 4). On both dynamic and isometric tasks, Model 8-tasks predicted net joint moment with a mean RMS_{error} of 6.11 (± 4.41 N.m) and a mean R^2 of 0.67 (± 0.26) (Table II).

[Insert Table II]

[Insert figure 4]

Estimation of the contributions of the plantarflexor and dorsiflexor muscle groups to the net joint moment

The contributions of the plantar flexor and dorsiflexor muscle groups to the net joint moment were significantly different between the Model 8-tasks, calibrated on all eight tasks, and both Model 2-tasks and Model RAB, which were calibrated on two dynamic tasks only ($F_{2,18}=13.95$; $p<0.05$ for the dorsiflexor and $F_{2,18}=13.87$; $p<0.05$ for the plantar flexor). Post-Hoc tests showed that the Model 8-tasks presented higher

peak values of dorsiflexor muscular moments (4.69 N.m ± 4.36 N.m) than Model 2-tasks (0.59 ± 0.82 N.m) and Model RAB (1.88 N.m ± 1.55 N.m). The plantar flexor muscular moments depended also on *models* with M_{PF} peak values for Model 8-tasks (-29.81 N.m ± 22.77 N.m) smaller than those of Model 2-tasks (-25.70 N.m ± 20.41 N.m) and Model RAB (-27.00 N.m ± 20.26 N.m).

DISCUSSION

The aim of this study was to develop a method for the clinicians to estimate the contributions of the agonist and antagonist muscle groups to the net ankle joint moment during both isometric and dynamic muscle contractions. The proposed model was designed to be applicable for clinical studies through the use of reduced and various experimental tasks without reducing the physiological correctness. From Model RAB[32], improvements were made to better account for physiologic phenomenon such as the electromechanical delay, and the non-linear force-length-velocity relationship and moment arm. The influence of these physiological changes on the moment prediction ability of the model was shown by an increase in R^2 values.

Following a calibration procedure, the modified model (Model 8-tasks & Model 2-tasks) was able to predict joint moments, and showed better prediction capacities than the Model RAB. Concerning the net joint moment prediction capabilities on both dynamic and isometric conditions, the modified model showed similar results compared to the previous studies that aimed at estimating the contributions of individual muscles or opposing muscle groups to the net joint moment. The accuracy of this model for net joint moment prediction was within the range of other studies [9,21,24] where RMS_{error} were among the lowest values (6.1N.m ± 4.4). The mean value for the coefficient of determination (R^2) was 0.64 over all tasks, and when considering the isometric tasks only, the R^2 value (0.74) was similar to Laursen et al.[24] and in the range of results presented by Kellis and Katis [21]. However, the ability to predict net moment remained lower than results obtained by Lloyd and Besier [26] with R^2 values of 0.91. These differences could be explained by a more complete description of the physiological process responsible of force production in

the EMG-driven model proposed by Lloyd and Besier [26]. Indeed, there is a trade-off between physiological correctness and improved accuracy, but it comes at the expense of making it more difficult to implement in a clinical setting.

The improved predictive ability of the modified model (Model 8-tasks & Model 2-tasks) compared to the Model RAB could result from the inclusion of additional physiological muscle properties. First, several models incorporated the EMD either by a recursive filter[4] or a single pass filter[10] whereas in the Model RAB, a zero-lag filter was used to remove the temporal shift introduced by filtering. In this study, the mean value of EMD was 83.6 ms and similar results were obtained for knee flexors[30] and arm muscles[17]. The EMD could depend on several factors such as muscle stiffness [14], the tendon slack length [30], and the computation method [17], highlighting the importance of taking differences into account when estimating the EMD. In the present study, EMD was estimated and introduced during EMG processing according to the method described by [29] without adding complexity to the model implementation. The second improvement of the modified model was the integration of a non-linear force-length-velocity relationship [13,34] with subject specific anthropometric data as input (muscles fiber lengths, muscle fiber velocities, and moment arms). All these parameters were introduced using a single parameter representing the capacity of muscle moment production. We found that the corresponding values for the gastrocnemii were smaller in the seated position than in the upright position and that soleus values were higher than the gastrocnemii in the seated position. These results were in agreement with other studies [19,27] that indicated the ability of gastrocnemii force production was reduced for knee flexion angles above 90°. In the modified model, the use of an anatomical model to determine the muscle fiber lengths and moment arms allows one to take into account more accurately the influences of different joint angles and subject's differences on muscle-tendon characteristics.

The influence of the types of calibration tasks has been shown on the model parameters. The α factor was significantly different between the Model 8-tasks and the Model 2-tasks. Moreover, the modified model calibrated on eight tasks (Model 8-tasks) and only on two dynamic tasks (Model 2-tasks)

showed differences in the estimations of the contributions of the dorsiflexor and plantar flexor muscle groups to the net joint moment. Indeed, M_{DF} which represented the contribution of antagonist muscle group to the net joint moment was lower when the models were calibrated on dynamic tasks only (Model 2-tasks and Model RAB). These results showed that the estimation of contribution of agonist and antagonist muscle groups to the net joint moment was sensitive to the choice of muscle contraction types used for the calibration process (i.e., isometric and dynamic vs. dynamic only). Since the same muscle properties were used, different outputs could only be explained by the use of different calibration tasks with the calibration tasks used for the Model 8-tasks encompassing larger range of conditions compared to the Model 2-tasks. The use of various tasks seems to reduce the solution space for the adjustable model parameters. This assumption is strongly supported by previous papers. Indeed, Lloyd and Besier [26] argued that the use of large type of contractions and condition allows reducing the solution space for the optimized parameters to operate within physiological limits. This point is particularly seen in the current model when looking at the alpha factor that represents the isometric EMG-moment relationship. This parameter could be estimated using a constrained non-linear optimization scheme whatever the calibration tasks, even using dynamic tasks only as in the Model 2-tasks case. From our results, when alpha was estimated on dynamic tasks only, the value differed from calibration on isometric and dynamic tasks. The use of additional isometric tasks modified the estimation of the optimized parameters. As one of the tasks used in the calibration process was purely isometric for the Model 8-tasks, the resulting alpha parameter should be more representative of an EMG-moment relationship in isometric. Thus, we hypothesized that the use of dynamic tasks only seems to under-estimate the antagonist muscle group contribution to the net joint moment. The use of limited set of tasks (i.e. dynamic) could be detrimental to the correctness of the estimates of the contributions of the muscle groups to the net joint moment. As reported by Doorenbosch and Harlaar [10] for the EMG-force model to be successfully implemented as a clinical tool, the model has to be applied and evaluated for estimation muscle force for a wider range of muscular performances such as the model 8-tasks than just one type of contractions. Many studies use only isometric [21,23] or isokinetic [9] calibration

tasks. This study highlighted the importance of encompassing many different conditions during the calibration process, as recommended by Lloyd and Besier [26]. Increasing the number and types of calibration tasks may help the optimized parameters to be more representative of all the existing conditions of movement production. Thus, we chose to calibrate our model on both isometric and dynamic tasks with two extreme joint positions: seated and upright. Different angles at the knee joint were motivated by taking the two bi-articular muscles into account. Moreover, using the fewest number of calibration trials (isometric and dynamic) is a requirement for the models to be used in clinical settings. While Kellis and Katis calibrated and validated their model on 54 contractions [21], this study used only eight trials to calibrate the model and eight to predict muscle moments. The limited number of calibration trials seems convenient for use of this model in clinical studies where patients are involved.

The eight tasks used in this study were either at a high frequency of 1 Hz or either at near zero Hz for the ramp condition. The Model 8-tasks spans two extremes frequencies with good prediction. It would be interesting for further studies to test the model across different intermediate frequencies (such as walking with different speed, running) in order to validate this model as generalizable for any task.

One limitation of the present model is that the passive moment of muscle fibers due to the parallel elastic component of Hill-type model is neglected. This passive moment could probably be attributed to the elastic properties of the connective tissues between the muscle fibers, endomysium and epimysium [18] and intrafibrillar proteins such as titin [7]. Considering the range of ankle motion we hypothesized that these passive components were unsolicited. In addition, the ratio between the tendon length and muscle fiber length of the studied muscles is high, so the parallel elastic component could be neglected in regard to the compliance of the series component [41]. To implement the model on other tasks where the parallel elastic component is more likely to play a role, the passive force-length relationship should be modified. In addition, the modified model in its current form could be applied to any single DOF joint, but would need additional development for higher DOF joints.

The estimation of contribution of agonist and antagonist muscle groups to the net joint moment are

required to compute the co-contraction level [40]. This variable could not be estimated only from EMG because the muscle moment production depends on other factors such as force-length-velocity relationship and the moment arm of the muscle-tendon complex. The model proposed in this study allows taking into account these muscle properties to estimate the muscle groups contribution. The co-contraction level provides crucial information for clinicians to understand how the nervous system deals with the muscular redundancy for patients. Patients with musculoskeletal or neurologic disorders would use different muscle recruitment patterns from healthy subjects and could exhibit co-contraction levels different than healthy people. For example, the EMG-to-moment model presented in this study could be used to investigate the functional recovery following surgical treatment of Achilles' tendon rupture by a longitudinal study combined with other biomechanical parameters [8].

Compared to existing neuromusculoskeletal tracking models [36], one key point of the proposed model relies on the fact that the muscle activation patterns could be taken into account using EMG data as input to estimate the contribution of the agonist/antagonist muscle groups to the net joint moment. Moreover, and whereas patients are usually unable to perform maximum voluntary contractions, the EMG-to-moment model developed in this study didn't need MVIC to normalize EMG data compared to other studies [21], improving the accessibility of our model for clinical settings.

CONCLUSION

The proposed EMG-to-moment model was developed in order to be suitable for clinical studies. The physiological correctness incorporated in the proposed model concerned the electromechanical delay and a non-linear force-length-velocity relationship with subject's specific anthropometric data as input. Significant improvements in moment predictions across isometric and dynamic tasks were found relative to the Model RAB. The choice of different types of muscle contraction used for the calibration process influenced the estimation of the contributions of agonist and antagonist muscle groups to the net joint moment. From our results, the use of various calibration tasks (i.e., isometric and dynamic) allows to be

more confident in the estimation of the contribution of the muscle groups to the net joint moment. The resulting solution seems to be more within physiological limits. The proposed model is simpler than others and therefore may be more suitable for clinical studies. From this model, the contribution of agonist-antagonist muscle groups to the net joint moment could be estimated as well as the co-contraction index around a joint [40]. This information could be crucial when the biologic system is altered by musculoskeletal or neurologic disorders.

ACKNOWLEDGEMENTS

The authors whish to thank Dr. Laurent Vigouroux (Aix-Marseille University), and Kurt Manal (Department of Mechanical Engineering, University of Delaware, Newark, DE, USA) for their helpful comments on the manuscript.

REFERENCES

[1] Allinger, T. L. and J. R. Engsberg. A method to determine the range of motion of the ankle joint complex, in vivo. *J Biomech*, 26:69–76, 1993.

[2] Amarantini, D. and L. Martin. A method to combine numerical optimization and EMG data for the estimation of joint moments under dynamic conditions. *J Biomech*, 37:1393–1404, 2004.

[3] Buchanan, T. S.. Evidence that maximum muscle stress is not a constant : differences in specific tension in elbow flexors and extensors. *Med Eng Phys*, 17:529–536, 1995.

[4] Buchanan, T. S., D. G. Lloyd, K. Manal, and T. F. Besier. Neuromusculoskeletal modeling : estimation of muscle forces and joint moments and movements from measurements of neural command. *J Appl Biomech*, 20:367–395, 2004.

[5] Delp, S. L., F. C. Anderson, A. S. Arnold, P. Loan, A. Habib, C. T. John, E. Guendelman, and D. G. Thelen. Opensim : open-source software to create and analyze dynamic simulations of movement. *IEEE Trans Biomed Eng*, 54:1940–1950, 2007.

[6] Delp, S. L., J. P. Loan, M. G. Hoy, F. E. Zajac, E. L. Topp, and J. M. Rosen. An interactive graphics-based model of the lower extremity to study orthopaedic surgical procedures. *IEEE Trans Biomed Eng*, 37:757–767,1990.

[7] Denoth, J., E. Stüssi, G. Csucs, and G. Danuser. Single muscle fiber contraction is dictated by inter-sarcomere dynamics. *J Theor Biol*, 216:101–122, 2002.

[8] Don, R., A. Ranavolo, A. Cacchio, M. Serrao, F. Costabile, M. Iachelli, F. Camerota, M. Frascarelli, and V. Santilli. Relationship between recovery of calf-muscle biomechanical properties and gait pattern following surgery for achilles tendon rupture. *Clin Biomech*, 22:211–220, 2007.

[9] Doorenbosch, C. A. M., and J. Harlaar. A clinically applicable EMG-force model to quantify active stabilization of the knee after a lesion of the anterior cruciate ligament. *Clin Biomech*, 18:142–149, 2003.

[10] Doorenbosch, C. A. M., and J. Harlaar. Accuracy of a praticable EMG to force model for knee muscles. *Neuroscience Letters*, 368:78-81, 2004.

[11] Finni, T., P. V. Komi, and J. Lukkariniemi. Achilles tendon loading during walking : application of a novel optic fiber technique. *Eur J Appl Physiol Occup Physiol*, 77(3) :289–291, 1998.

[12] Fukunaga, T., R. R. Roy, F. G. Shellock, J. A. Hodgson, and V. R. Edgerton. Specific tension of human plantar flexors and dorsiflexors. *J Appl Physiol*, 80:158–165, 1996.

[13] Gordon, A. M., A. F. Huxley, and F. J. Julian. The variation in isometric tension with sarcomere length in vertebrate muscle fibres. *J Physiol*, 184:170–192, 1966.

[14] Granata, K. P., and W. S. Marras. Cost-benefit of muscle cocontraction in protecting against spinal instability. *Spine*, 25:1398–1404, 2000.

[15] Hermens, H. J., B. Freriks, C. Disselhorst-Klug, and G. Rau. Development of recommendations for sEMG sensors and sensor placement procedures. *J Electromyogr Kinesiol*, 10:361–374, 2000.

[16] Hill, A. V.. The heat of shortening and the dynamic constants of muscle. *Proceedings of the Royal Society of London. Series B, Biological Sciences*, 136:399, 1938.

[17] Hodges, P. W., and B. H. Bui. A comparison of computer-based methods for the determination of onset of muscle contraction using electromyography. *Electroencephalogr Clin Neurophysiol*, 101:511–519, 1996.

[18] Hof, A. L.. In vivo measurement of the series elasticity release curve of human triceps surae muscle. *J Biomech*, 31:793–800, 1998.

[19] Hof, A. L., and J. van den Berg. Linearity between the weighted sum of the EMGs of the human triceps surae and the total torque. *J Biomech*, 10:529–539, 1977.

[20] Howatson, G., M. Glaister, J. Brouner, and K. A. van Someren. The reliability of electromechanical delay and torque during isometric and concentric isokinetic contractions. *J Electromyogr Kinesiol*, 19:975-979, 2008.

[21] Kellis, E,. and A. Katis. Hamstring antagonist moment estimation using clinically applicable models : Muscle dependency and synergy effects. *J Electromyogr Kinesiol*, 18:144–153, 2008.

[22] Krevolin, J. L., M. G. Pandy, and J. C. Pearce. Moment arm of the patellar tendon in the human knee. *J Biomech*, 37:785–788, May 2004.

[23] Langenderfer, J., S. LaScalza, A.Mell, J. E. Carpenter, J. E. Kuhn, and R. E. Hughes. An EMG-driven model of the upper extremity and estimation of long head biceps force. *Comput Biol Med*, 35:25–39, 2005.

[24] Laursen, B., B. R. Jensen, G. Németh, and G. Sjøgaard. A model predicting individual shoulder muscle forces based on relationship between electromyographic and 3d external forces in static position. *J Biomech*, 31:731–739, 1998.

[25] Linford, C.W., J. T. Hopkins, S. S. Schulthies, B. Freland, D. O. Draper, and I. Hunter. Effects of neuromuscular training on the reaction time and electromechanical delay of the peroneus longus muscle. *Arch Phys Med Rehabil*, 87:395–401, 2006.

[26] Lloyd, D., and T. Besier. An EMG-driven musculoskeletal model to estimate muscle forces and knee joint moments in vivo. *J Biomech*, 36 :765–776, 2003.

[27] Maganaris, C. N. Force-length characteristics of in vivo human skeletal muscle. *Acta Physiol Scand*, 172 :279–285, 2001.

[28] Manal, K., and T. S. Buchanan. A one-parameter neural activation to muscle activation model : estimating isometric joint moments from electromyograms. *J Biomech*, 36:1197–1202, 2003.

[29] Manal, K., and W. Rose. A general solution for the time delay introduced by a low-pass butterworth digital filter : An application to musculoskeletal modeling. *J Biomech*, 40:678–681, 2007.

[30] Muraoka, T., T. Muramatsu, T. Fukunaga, and H. Kanehisa. Influence of tendon slack on electromechanical delay in the human medial gastrocnemius in vivo. *J Appl Physiol*, 96:540–544, 2004.

[31] Nussbaumand, M. A., D. B. Chaffin. Lumbarmuscle force estimation using a subject-invariant 5-parameter EMG-based model. *J Biomech*, 31:667–672, 1998.

[32] Rao, G., D. Amarantini, and E. Berton. Influence of additional load on the moments of the agonist and antagonist muscle groups at the knee joint during closed chain exercise. *J Electromyogr Kinesiol*, 19:459–466, 2009.

[33] Riener, R., and T. Edrich. Identification of passive elastic joint moments in the lower extremities. *J Biomech*, 32:539–544, 1999.

[34] Schutte, L., M. Rodgers, F. Zajac, and R. Glaser. Improving the efficacy of electrical stimulation-induced leg cycle ergometry: an analysis based on a dynamic musculoskeletal model. *IEEE Trans. Rehab. Eng.*, 1:109–125, 1993.

[35] Scott, S. H., and G. E. Loeb. Mechanical properties of aponeurosis and tendon of the cat soleus muscle during whole-muscle isometric contractions. *J Morphol*, 224:73–86, Apr 1995.

[36] Seth, A., and M. G. Pandy. A neuromusculoskeletal tracking method for estimating individual muscle forces in human movement. *J Biomech*, 40:356–366, 2007.

[37] Shiavi, R., C. Frigo, and A. Pedotti. Electromyographic signals during gait: criteria for envelope filtering and number of strides. *Med Biol Eng Comput*, 36:171–178, 1998.

[38] Solomonow, M., R. Baratta, B. H. Zhou, H. Shoji, W. Bose, C. Beck, and R. D'Ambrosia. The synergistic action of the anterior cruciate ligament and thigh muscles in maintaining joint stability. *Am J Sports Med*, 15:207–213, 1987.

[39] Van Dieën, J. H., and B. Visser. Estimating net lumbar sagittal plane moments from EMG data. the validity of calibration procedures. *J Electromyogr Kinesiol*, 9:309–315, 1999.

[40] Winter, D. A. Biomechanics andMotor Control of HumanMovement. Wiley, second edition, 1990.

[41] Zajac, F. E. Muscle and tendon : properties, models, scaling, and application to biomechanics and motor control. *Crit Rev Biomed Eng*, 17:359–411, 1989.

[42] Zatsiorky, V., and V. Seluyanov. Biomechanics VIII-B Chapitre The mass and inertial characteristics of mains segments of the human body. Human Kinetcis Champaign, pp. 1152-1159, 1983.

Tables

Table I

Input parameters for the Model 8-tasks, Model 2-tasks, and Model RAB.

Type of variable	Symbol of variable	Description of variable	Model 8-tasks & Model 2-tasks	Model RAB	Related element	Range of variation
Optimized parameters	α_i	Linear isometric moment-EMG relationship	x	x	Muscle	$\lvert\alpha_i\rvert > 0$
	$w_i\ (t)$	Relative contribution of each muscle to the total moment of muscle group	x	x	Muscle	$0 < w_i\ (t) < 1$
	G_l	Gain of each muscle group	*x*		Muscle group	$0.5 < \lvert G_l\rvert < 2$
	βj	Linear moment-angle effect		x	Joint	$Bj>0$
	δj	Linear moment-velocity effect		x	Joint	$\delta j>0$
Experimental data	$fEMG_i(t)$	Full-wave rectified, filtered and temporally shifted EMG	x		Muscle	
	$rEMG_i(t)$	Full-wave rectified, filtered EMG		x	Muscle	
Experimental data Opensim Theoretical relationships	$\bar{\varphi}_i(t) = \bar{\gamma}_i(t).\bar{d}_i(t)$	Normalized capacity of muscle moment production	x		Muscle	
	$\bar{\gamma}_i(t) = \bar{f}(v_i(t)).\bar{f}((l_i(t))$	Normalized capacity of muscle force production	x		Muscle	
	$\bar{f}((l_i(t))$	Normalized active force-length relationship	x		Muscle	$0 < \bar{f}((l_i(t)) < 1$
	$\bar{f}(v_i(t))$	Normalized force-velocity relationship	x		Muscle	$0 < \bar{f}((v_i(t)) < 1.8$
	$\bar{d}_i(t)$	Normalized moment arm	x		Muscle	$0 < \bar{d}_i(t) < 1$

Table II

Summary of Models Predictions according to different tasks.

		Dynamic		Isometric					
		Seated	Upright	Seated			Upright		
				10-30	30-50	Ramp	10-30	30-50	Ramp
R^2	Model 8-tasks	0.38 ± 0.24	0.53 ± 0.25	0.83 ± 0.28	0.81 ± 0.21	0.65 ± 0.25	0.75 ± 0.21	0.80 ± 0.14	0.60 ± 0.22
	Model 2 -tasks	0.46 ± 0.2	0.60 ± 0.25	-	-	-	-	-	-
	Model RAB	0.18 ± 0.19	0.39 ± 0.26	-	-	-	-	-	-
RMS_{error} (N.m)	Model 8-tasks	2.77 ± 2.09	4.60 ± 1.74	2.93 ± 6.21	6.64 ± 3.40	5.98 ± 2.09	6.64 ± 3.40	6.67 ± 2.92	10.78 ± 1.95
	Model 2-tasks	1.80 ± 1.35	5.18 ± 4.04	-	-	-	-	-	-
	Model RAB	1.62 ± 0.78	7.26 ± 4.25	-	-	-	-	-	-

Figure legends

FIGURE 1

Experimental apparatus used for the isometric conditions. Note that the subject was restrained (a) at the shoulder level for the upright position and (b) at the knee level for the seated position.

FIGURE 2

Mean value of the variable φ representing the capacity of muscle moment production for all muscles estimated from a generic force-length-velocity relationship and experimental data. † and * indicate significant effects ($p<0.05$) of the position and muscle factors, respectively.

FIGURE 3

Comparison of the ankle net joint moment predicted on dynamic tasks by inverse dynamics, Model 8-tasks, Model 2-tasks and Model RAB for one subject (a) seated position and (b) upright position. Note the highest prediction capacity of the modified model proposed in this paper compared to the Model RAB.

FIGURE 4

Comparison of the ankle net joint moment predicted by the Model 8-tasks and net joint moment computed by inverse dynamics for one subject on isometric tasks. Note the shape similarity between both datasets.

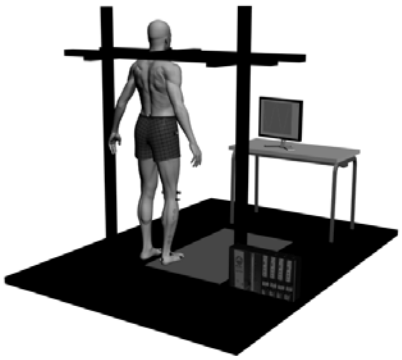

(a)

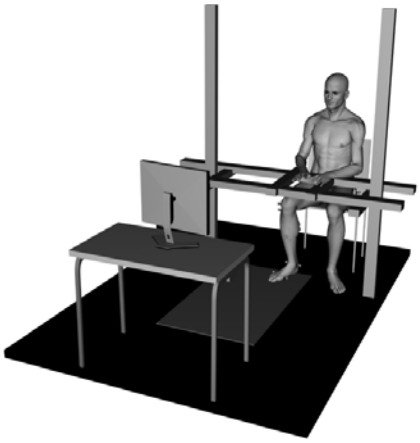

(b)

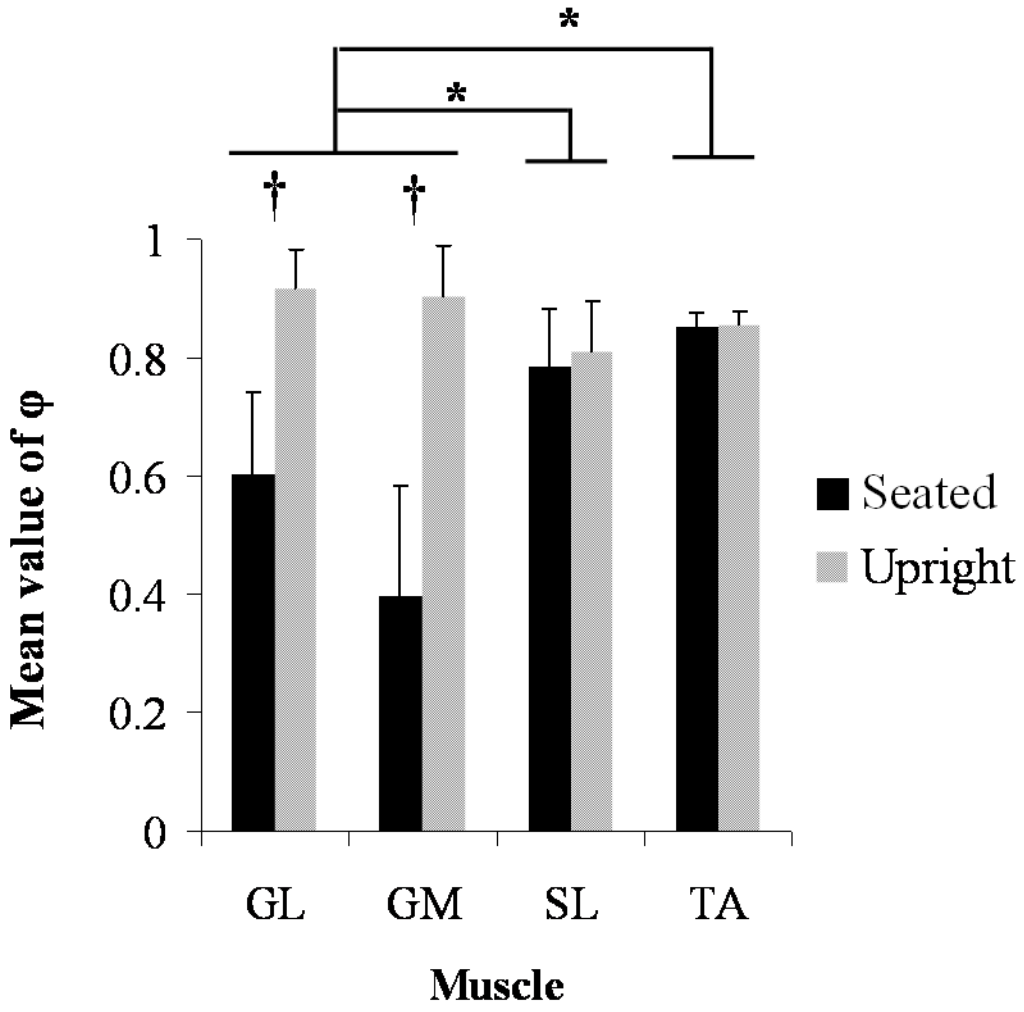
*
*
†
†
1
0.8
0.6
0.4
0.2
0
Mean value of φ
GL
GM
SL
TA
Muscle
Seated
Upright

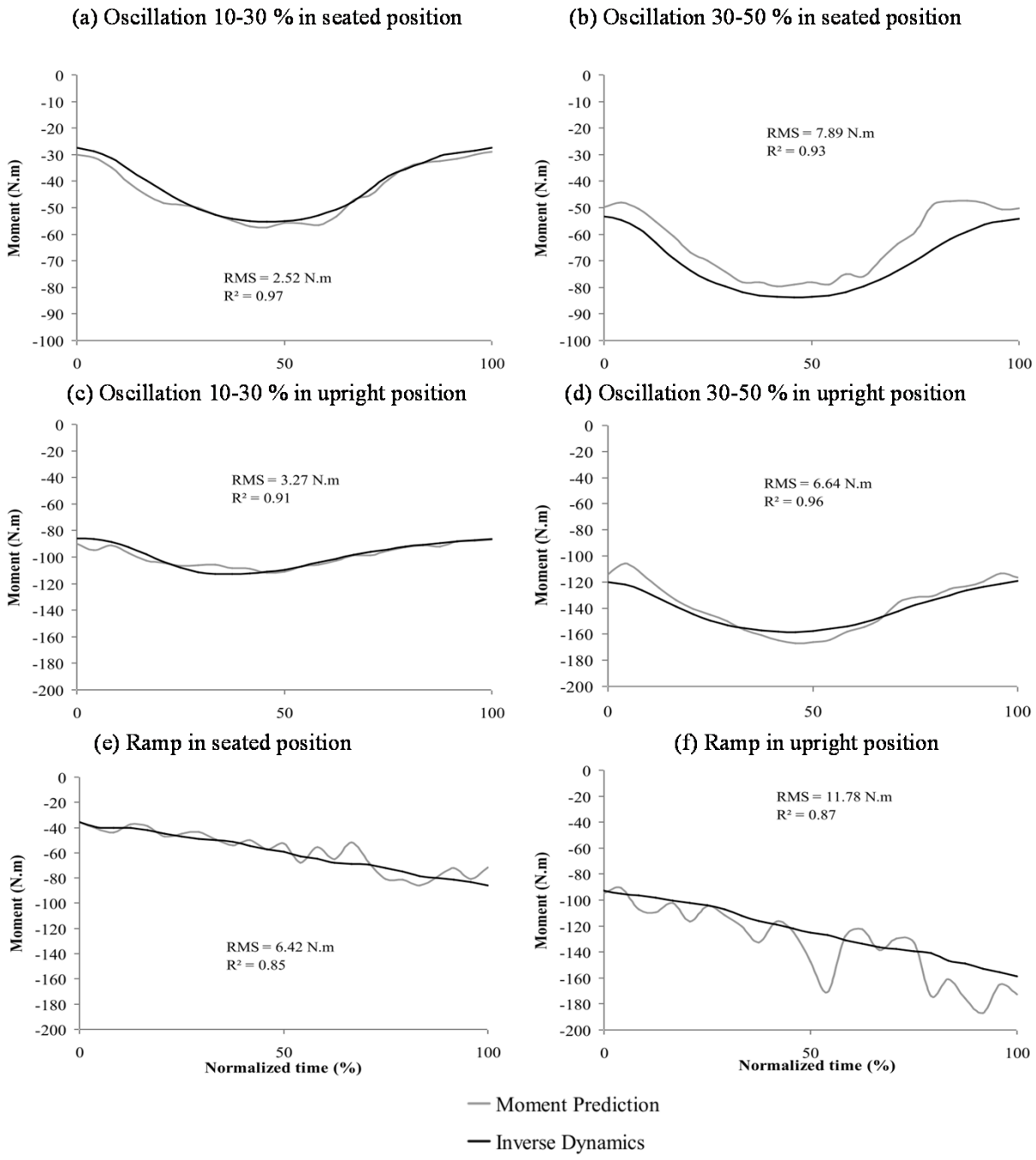
(a) Oscillation 10-30 % in seated position
(b) Oscillation 30-50 % in seated position
(c) Oscillation 10-30 % in upright position
(d) Oscillation 30-50 % in upright position
(e) Ramp in seated position
(f) Ramp in upright position
Moment (N.m)
RMS = 2.52 N.m
R² = 0.97
RMS = 7.89 N.m
R² = 0.93
RMS = 3.27 N.m
R² = 0.91
RMS = 6.64 N.m
R² = 0.96
RMS = 6.42 N.m
R² = 0.85
RMS = 11.78 N.m
R² = 0.87
Normalized time (%)
Moment Prediction
Inverse Dynamics

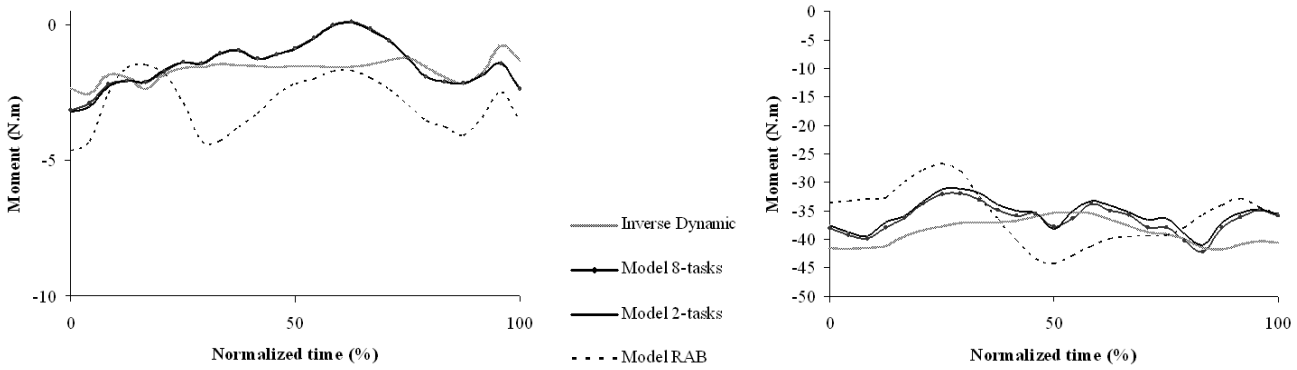
0
-5
-10
Moment (N.m)
0
50
100
Normalized time (%)
Inverse Dynamic
Model 8-tasks
Model 2-tasks
Model RAB
0
-5
-10
-15
-20
-25
-30
-35
-40
-45
-50
Moment (N.m)
0
50
100
Normalized time (%)